J. Plasma Physics (2012), *vol.* 78, *part* 1, *pp.* 47–54. © Cambridge University Press 2011
doi:10.1017/S0022377811000407

Empirical versus exact numerical quasilinear analysis of electromagnetic instabilities driven by temperature anisotropy

PETER H. YOON[1,2], JUNG JOON SEOUGH[1], KHAN HYUK KIM[1] and DONG HUN LEE[1]

[1]School of Space Research, Kyung Hee University, Yongin-Si, Gyeonggi-Do, 446-701, South Korea (yoonp@umd.edu)

[2]Institute for Physical Science and Technology, University of Maryland, College Park, MD 20742, USA

(Received 29 July 2011; revised 21 August 2011; accepted 1 September 2011; first published online 29 September 2011)

Abstract. In the present paper, quasilinear development of anisotropy-driven electromagnetic instabilities is computed on the basis of recently formulated empirical wave dispersion relation and compared against exact numerical calculation based upon transcendental plasma dispersion function and exact numerical roots. Upon comparison with the exact method it is demonstrated that the empirical model provides reasonable results. The present findings may be relevant to space physical application, as the present paper provides a useful short-cut research method for self-consistent analysis of temporal development of anisotropy-driven instabilities.

1. Introduction

Modeling the sources and losses of Earth's radiation belt electrons is an important research topic in contemporary space plasma physics. One of the most important theoretical tools for such an effort is based on quasilinear theory, which has been employed since the 1960s (Kennel and Petschek 1966; Lyons et al. 1972; Schulz and Lanzerotti 1974; Summers and Ma 2000; Summers and Thorne 2003; Albert 2005; Glaubert and Horne 2005; Summers 2005; Summers et al. 2007; Xiao et al. 2010). However, one of the key assumptions in such an undertaking is that the waves are described by the cold plasma theory.

It is plausible that the radiation belts are characterized by finite plasma betas, especially during storm times. Although direct measurements of plasma betas in the inner magnetosphere is not straightforward, there are some published estimates of the inner magnetospheric plasma betas that indicate that plasma betas in the radiation belt, ring current, and the inner magnetosphere can be quite substantial during disturbed conditions. For instance, Lui et al. (1987) investigated the development of radial profiles of the plasma beta, perpendicular and parallel pressures, current densities in the storm time ring current based on AMPTE spacecraft data. They found that the ring current plasma beta could increase to an order 1 value. They also showed that the pressure anisotropy $P_\perp/P_\parallel$ could be as high as $\sim$3 to $\sim$5 during the peak of the storm time. This shows that the finite beta effects and pressure or temperature anisotropy cannot be ignored for the storm time ring current and radiation belts, especially for the outer belts.

It is well known that the plasma dispersion relation for finite betas can deviate substantially from the cold-plasma solution. Nevertheless, cold plasma theory has been invariably used in the radiation belt transport coefficient calculations because hot/warm plasma (or finite beta) dispersion relation makes the calculation intractable. Within the definition for the quasilinear diffusion coefficients lies the relativistic wave-particle cyclotron resonance condition,

$$0 = \omega - k_\parallel v_\parallel - n\Omega_e/\gamma,$$

where ω is the wave frequency, $k_\parallel$ stands for the parallel wave number, $\Omega_e = eB/mec$ is the electron cyclotron frequency defined with respect to the rest mass of the electron, and $\gamma = (1 - v^2/c^2)^{-1/2}$ is the relativistic mass (Lorentz) factor. In order to evaluate the above resonance condition one must provide a closed form expression for the wave dispersion relation, $\omega = \omega(k_\parallel)$ or $k_\parallel = k_\parallel(\omega)$, say in the case of parallel propagation. In the case of cold plasma such a relation is readily available. However, for warm/hot plasmas the dispersion relation must be generally computed on the basis of transcendental dispersion function, which makes the computation of resonant $k_\parallel$ impractical if not intractable. This is the reason why cold plasma models are used in the literature for the wave dispersion relation.

In a recent series of papers (Seough and Yoon 2009; Yoon et al. 2010, 2011) the authors analytically modeled the numerical warm plasma dispersion relations for both left- and right-hand circularly polarized electromagnetic waves propagating parallel to the ambient magnetic field. Specifically, Seough and Yoon (2009) discussed the empirical models for the right-/left-hand circularly polarized waves in isotropic thermal plasmas. Yoon et al. (2010) discussed the empirical model of low-frequency electromagnetic ion-cyclotron (EMIC) instability driven by temperature anisotropy, while Yoon et al. (2011) extended the discussion to whistler anisotropy instability.

https://doi.org/10.1017/S0022377811000407 Published online by Cambridge University Press

In all these papers empirical models and exact numerical solutions were compared and it was found that both the real frequency and growth rate compared reasonably well against actual numerical roots.

The significance of our recent works (Seough and Yoon 2009; Yoon et al. 2010, 2011) is that the closed-form analytical nature associated with the empirical dispersion formulae could finally make it possible for one to include warm plasma effects in the radiation belt transport coefficient calculation. Before we do that, however, it is important to address the following issue: Given that the empirical dispersion formulae are not exact solutions and some discrepancies are bound to exist, will small differences accumulate and amount to large deviations in the long run over the course of nonlinear instability development? To address this issue, we perform quasilinear analysis on the basis of the empirical formula as well as more rigorous numerical analysis first developed by Davidson and Ogden (1975), and compare the outcomes.

Upon comparing the present approach against the actual numerical solution, we find that our results are in good agreement, which means that the empirical approach to anisotropy-driven electromagnetic instability problem can be a useful shortcut tool that can be applied for studying long-time evolution of EMIC or whistler anisotropy instability. In the remainder of the present paper we discuss our methodology and findings in detail. The organization of the paper is as follows: In Sec. 2 we briefly review the linear theory of EMIC and whistler waves and instabilities, as well as empirical models thereof. In Sec. 3 we discuss quasilinear theory of EMIC and whistler instability and present numerical results. Finally, in Sec. 4 we conclude the present paper. The content of Sec. 2 is largely the recapitulation of Yoon et al. (2010, 2011). However, for the sake of completeness as well as to properly set up the discussion in Sec. 3, which is new, we summarize the essential findings of the two previous papers (Yoon et al. 2010, 2011).

2. Linear theory

The dispersion relation for the right-/left-hand circularly polarized electromagnetic waves propagating parallel to the ambient magnetic field is given in standard form (Krall and Trivelpiece 1973; Davidson and Ogden 1975):

$$\frac{c^2k^2}{\omega^2} = 1 + \sum_a \frac{\omega_{pa}^2}{\omega^2} \int d\mathbf{v}\, \frac{v_\perp/2}{\omega - kv_\parallel \pm \Omega_a} \times \left((\omega - kv_\parallel)\frac{\partial F_a}{\partial v_\perp} + kv_\perp \frac{\partial F_a}{\partial v_\parallel} \right), \qquad (2.1)$$

where (ω, k) stands for angular frequency – wave number pair, c is the speed of light *in vacuo*, species label $a = i, e$ stands for ions (protons) and electrons, respectively, and $\omega_{pa}^2 = 4\pi n e_a^2/m_a$ and $\Omega_a = e_a B/m_a c$ are squares of the plasma frequency and cyclotron frequency, defined with respect to species a, respectively. Here e_a represents the electric charge ($= e$ or $-e$ depending on whether $a = i$ or $a = e$), m_a stands for the particle mass, $B =$ constant is the magnetic field intensity associated with the ambient field, and F_a corresponds to the velocity space particle distribution function (normalized to unity, $\int d\mathbf{v}\, F_a = 1$). In (2.1) the upper/lower sign corresponds to the right-/left-hand circularly polarized waves (whistler or electromagnetic ion–cyclotron waves, respectively).

We are interested only in the slow (or subluminal) mode characterized by $ck/\omega > 1$. Hence, we may ignore the displacement current term, i.e. the unity on the right-hand side of (2.1). For anisotropic distribution with a Maxwellian parallel distribution $F_a = \sqrt{m_a/(2\pi T_{\parallel a})}\, G(v_\perp) \exp[-m_a v_\parallel^2/(2\pi T_{\parallel a})]$, where $G(v_\perp)$ is an arbitrary function, and $T_{\parallel a}$ is the parallel temperature, (2.1) reduces to (Davidson and Ogden 1975)

$$c^2k^2 = \sum_a \omega_{pa}^2 \left[\frac{\omega}{kv_{Ta}} Z(\zeta_\pm) + \left(\frac{T_{\perp a}}{T_{\parallel a}} - 1 \right) [1 + \zeta_\pm Z(\zeta_\pm)] \right], \qquad (2.2)$$

where $\zeta_\pm = (\omega \pm \Omega_a)/kv_{Ta}$, $T_{\perp a} = \pi m_a \int_0^\infty dv_\perp v_\perp^3 G(v_\perp)$ is the effective perpendicular temperature, and $v_{Ta} = (2T_{\parallel a}/m_a)^{1/2}$ is the parallel thermal speed. In the present paper we use temperatures defined in the unit of eV. As a consequence, the temperature is defined without the Boltzmann constant. Here $Z(\zeta) = \pi^{-1/2} \int_{-\infty}^{\infty} dx\, e^{-x^2} (x - \zeta)^{-1}$ is the Fried–Conte plasma dispersion function.

2.1. Electromagnetic ion-cyclotron (EMIC) instability

Let us first consider the case of lower sign (left-hand circular polarization). Such a case supports low-frequency waves characterized by $\omega < \Omega_i \ll |\Omega_e|$. In (2.2), the electron response can thus be simplified by assuming isotropy and 'cold' temperature, i.e. $T_{\perp e}/T_{\parallel e} = 1$ and $v_{Te} \to 0$. Upon making use of the inequality $\omega \ll |\Omega_e|$, (2.2) further reduces to (Davidson and Ogden 1975)

$$0 = \kappa^2 + x - A - \frac{(A+1)x - A}{\kappa \beta_\parallel^{1/2}} Z(\zeta), \quad \zeta = \frac{x-1}{\kappa \beta_\parallel^{1/2}}, \qquad (2.3)$$

where $x = \omega/\Omega_i$ is normalized complex frequency, $\kappa = ck/\omega_{pi} = kv_A/\Omega_i$ is normalized wave number, where $v_A = B/(4\pi n m_i)^{1/2}$ stands for Alfvén speed, $A = T_{\perp i}/T_{\parallel i} - 1$ represents the temperature anisotropy factor, and $\beta_\parallel = 8\pi n T_{\parallel i}/B^2$ stands for parallel ion beta. Following previous studies (Davidson and Ogden 1975), the real frequency and wave number corresponding to the marginal stability are given by

$$x_0 = A/(A+1), \quad \kappa_0^2 = A^2/(A+1) = Ax_0. \qquad (2.4)$$

As (2.3) shows, the linear wave and instability depend parametrically only on two dimensionless quantities, namely the temperature anisotropy factor A and the parallel ion beta $\beta_\parallel$.

Yoon et al. (2010) heuristically constructed an empirical model of the dispersion relation that agrees reasonably with exact numerical solution over a sufficiently wide range of A and $\beta_\parallel$. Their empirical model of the

https://doi.org/10.1017/S0022377811000407 Published online by Cambridge University Press

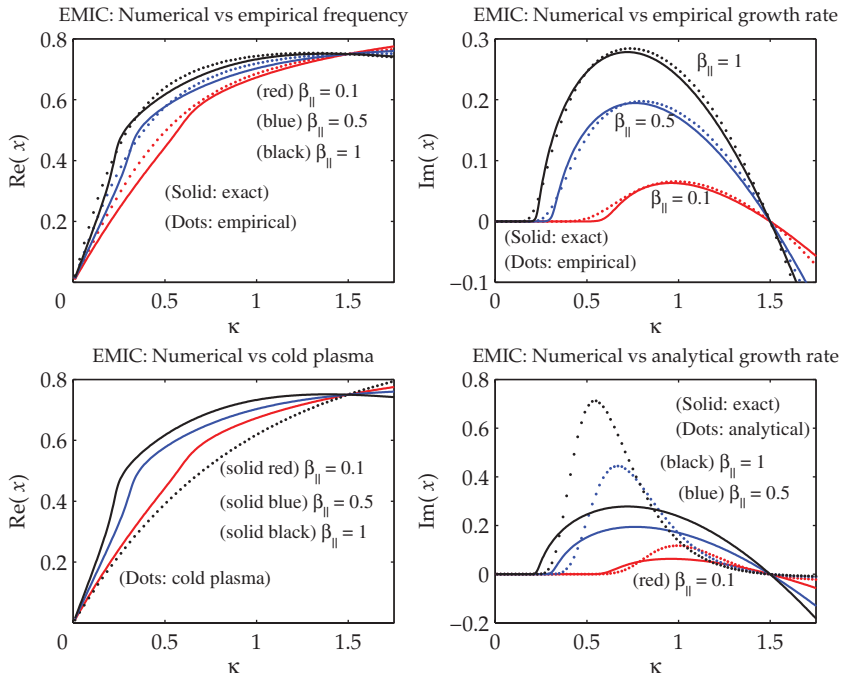


Figure 1. (Colour online) EMIC instability. (Top left): Comparison of exact numerical real frequency (solid lines), $\mathrm{Re}(x) = \omega/\Omega_i$, and empirical formula (dots) versus normalized wave number, $\kappa = kv_A/\Omega_i$, for anisotropy $A = T_\perp/T_\parallel - 1 = 3$ and for parallel betas, $\beta_\parallel = 8\pi n T_\parallel/B^2 = 0.1$ (red), 0.5 (blue), and 1 (black). (Top right): Comparison of exact numerical growth rate (solid lines), $\mathrm{Im}(x) = \gamma/\Omega_i$, and empirical formula (dots) versus normalized wave number, $\kappa = kv_A/\Omega_i$. (Bottom left): Comparison of exact roots and cold-plasma dispersion relation (dots). Note that an arguable agreement between the exact and approximate roots is found only for $\beta_\parallel = 0.1$. (Bottom right): Comparison of exact growth rate (solid lines) and analytical growth rate (dots). Note that approximate growth rate formula grossly overestimates the actual wave growth rate.

real frequency-associated EMIC instability is given by

$$\mathrm{Re}\,(x) = \frac{HG|\kappa|}{(1+D\kappa^2)^{1/2}}, \qquad D = 1 + 5\beta_\parallel^{3/2} + 2\beta_\parallel^{1/4},$$

$$H = \left(\frac{1+D\kappa_0^2}{A+1}\right)^{1/2},$$

$$G = 0.05\,\kappa^2\beta_\parallel(\kappa_0^2 - \kappa^2)e^{-|\kappa|} + 1, \tag{2.5}$$

where $\kappa_0^2 = A^2/(A+1)$ is defined in (2.4). For isotropic plasmas (2.5) reduces to the relation derived by Seough and Yoon (2009). The empirical model of the growth rate for EMIC instability driven by the temperature anisotropy is given by Yoon et al. (2010):

$$\mathrm{Im}\,(x) = \gamma_0\,|\kappa|^{1/2}\left(\kappa_0^2 - \kappa^2\right)\,\exp\left(-0.3\,\frac{[\mathrm{Re}\,(x)-1]^2}{\kappa^2\beta_\parallel}\right),$$

$$\gamma_0 = \frac{0.37\tanh(1.6A)}{\sqrt{A+0.01}}\,\frac{\beta_\parallel^p}{1+0.05\beta_\parallel^q},$$

$$p = 0.4e^{-A} + 0.46, \quad q = e^{-0.7A} + 1.5. \tag{2.6}$$

The empirical formulae (2.5) and (2.6) were compared against actual numerical roots over a range of input parameters, $1 < A < 10$ and $0 < \beta_\parallel < 2$, or so on. The results can be found in the paper by Yoon et al. (2010), where one can see that the agreement is quite reasonable. Here we reproduce one such comparison for the sake of completeness.

In Fig. 1 (top left) we show the real frequency $\mathrm{Re}(x)$ for the case of $A = 3$ and $\beta_\parallel$ ranging from 0.1 (red) to 0.5 (blue) to 1 (black). The exact numerical roots are plotted with solid lines, while empirical formula (2.5) is shown with dots. As one can see, the agreement between the exact and approximate roots is quite satisfactory. Similarly, in Fig. 1 (top right) we show the growth rate $\mathrm{Im}(x)$ for the same case of $A = 3$ and $\beta_\parallel$ ranging from 0.1 (red) to 0.5 (blue) to 1 (black). The exact numerical growth rates are plotted with solid lines, while empirical formula (2.6) is shown with dots. Again, the agreement between the exact and approximate growth rates is rather good.

In contrast with the empirical approach if we were to resort to the customary analytical dispersion relation and growth rate formula based upon asymptotic expansion of the Z function (e.g. Cuperman et al. 1975), then one would obtain

$$\mathrm{Re}(x) = \kappa\sqrt{1+\frac{\kappa^2}{4}} - \frac{\kappa^2}{2},$$

$$\mathrm{Im}(x) = -\sqrt{\pi}\,\frac{[\mathrm{Re}(x)-1]^2[\kappa^2 + \mathrm{Re}(x) - A]}{\kappa^2 + 2\mathrm{Re}(x)}$$

$$\times\,\frac{\exp\{-[\mathrm{Re}(x)-1]^2/\kappa^2\beta_\parallel\}}{\kappa\beta_\parallel^{1/2}}. \tag{2.7}$$

https://doi.org/10.1017/S0022377811000407 Published online by Cambridge University Press

However, the validity of the above approximation is extremely limited. If we employ approximate real frequency (i.e. the cold-plasma dispersion relation) and analytical growth rate formula shown in (2.7), then the results are as shown in bottom two panels of Fig. 1. In the bottom-left panel we show the exact real frequency Re(x) obtained numerically using solid lines as before, for the same set of input parameters as in Fig. 1, namely $A = 3$ and $\beta_\parallel$ ranging from 0.1 (red) to 0.5 (blue) to 1 (black), and compare the result against the cold dispersion relation shown in (2.7). As one can see, an arguable agreement between the exact and cold-plasma roots can be obtained only for $\beta_\parallel = 0.1$, but for higher parallel betas the exact roots deviate substantially from the cold-plasma dispersion relation. The situation is even worse for the growth rate. Displayed in Fig. 1 (bottom right) are exact growth rates shown in solid lines as before, and analytical growth rate formula based on (2.7). As one can see, the analytical growth rate formula grossly overestimates the wave growth. In general, the analytical formula (2.7) is valid only for extremely low $\beta_\parallel$ and for marginal stability $A \simeq 1$. This is the reason why empirical dispersion relation and growth rate formula were modeled by Seough and Yoon (2009) and Yoon et al. (2010).

2.2. Whistler anisotropy instability

In the case of right-hand circularly polarized electromagnetic perturbation propagating parallel/anti-parallel to the ambient magnetic field, we may ignore ion response in (2.2) and proceed to write the dimensionless form of the dispersion relation

$$0 = \kappa^2 - A - \frac{(A+1)\,x - A}{\kappa \beta_\parallel^{1/2}}\, Z\left(\frac{x-1}{\kappa \beta_\parallel^{1/2}}\right), \qquad (2.8)$$

where $x = \omega/|\Omega_e|$ is now the frequency normalized with respect to the electron cyclotron frequency, $\kappa = ck/\omega_{pe}$ represents the wave number normalized with respect to the electron skin depth, $A = T_{\perp e}/T_{\parallel e} - 1$ is the temperature anisotropy factor associated with the electrons, and $\beta_\parallel = 8\pi n T_{\parallel e}/B^2$ corresponds to the electron beta. The reader should not be confused with same notations used in (2.3) where the normalizations were done with respect to the ion quantities. Just as in the case of EMIC instability, the real frequency and wave number corresponding to the marginal whistler instability can be shown to be

$$x_0 = A/(A+1), \quad \kappa_0^2 = A. \qquad (2.9)$$

Yoon et al. (2011) obtained exact numerical solutions of (2.8), which is a standard practice, as well as an empirical model of numerical solutions that are valid over a limited but sufficiently broad range of parameter space, say for $1 < A < 10$ and $0 < \beta_\parallel < 3$ and so on. The model is given by

$$\mathrm{Re}\,(x) = \frac{HG\kappa^2}{1 + G\kappa^2[1 + \exp(-|\kappa|/2)\tanh(\beta_\parallel/0.06)]},$$

$$H = \frac{1 + GA[1 + \exp(-A^{1/2}/2)\tanh(\beta_\parallel/0.06)]}{G(A+1)},$$

$$G = 1 + A\tanh(2\beta_\parallel),$$

$$\mathrm{Im}\,(x) = P\beta_\parallel^Q \kappa^{1/2}(A - \kappa^2)\exp\left(-S\,\frac{[\mathrm{Re}\,(x)-1]^2}{\kappa^2\beta_\parallel}\right),$$

$$P = 0.16\,\frac{1 + \tanh[10\,(A-0.1)]}{A^{0.34} + 0.01},$$

$$Q = 0.5\tanh(1.5A), \quad S = 0.55\exp(-0.3A). \qquad (2.10)$$

In Fig. 2 (top left) we show the real frequency Re(x) for the case of $A = 3$ and $\beta_\parallel$ ranging from 0.1 (red) to 0.5 (blue) to 1 (black). The exact numerical roots are plotted with solid lines, whereas empirical formula (2.5) is shown with dots. As one can see, the agreement between the exact and approximate roots is quite satisfactory. The growth rate Im(x) for the same case of $A = 3$ and $\beta_\parallel$ ranging from 0.1 (red) to 0.5 (blue) to 1 (green) to 2 (black) is displayed in Fig. 2 (top right). The exact numerical growth rates are plotted with solid lines, whereas empirical formula (2.10) is shown with dots. As one can see, excellent agreement between the exact and approximate growth rates is found.

For the sake of completeness, we now repeat the customary treatment of the whistler anisotropy instability based upon cold plasma dispersion relation and the Landau growth rate formula that makes use of an asymptotic expansion of the Z function (e.g. Cuperman et al. 1975),

$$\mathrm{Re}(x) = \frac{\kappa^2}{1+\kappa^2},$$

$$\mathrm{Im}(x) = -\sqrt{\pi}\,\frac{[1 - \mathrm{Re}(x)]^2\,[(A+1)\,\mathrm{Re}(x) - A]}{\kappa\beta_\parallel^{1/2}}$$

$$\times \exp\left(-\frac{[\mathrm{Re}(x)-1]^2}{\kappa^2\beta_\parallel}\right). \qquad (2.11)$$

As with EMIC instability, the above approximation has an extremely limited range of validity. In order to demonstrate this, we show in Fig. 2 (bottom left) the exact real frequency Re(x) using solid lines and superpose the cold-plasma dispersion relation (2.11). As with the case of EMIC, good agreement is found only for $\beta_\parallel = 0.001$, which is expected, but for higher parallel betas the exact roots deviate substantially from the cold-plasma dispersion relation. Again, as in the case of EMIC instability, the discrepancy between the actual and analytical formulae is much worse for the growth rate. Plotted in Fig. 2 (bottom right) are exact growth rates shown in solid lines and analytical growth rate formula based on (2.11) in dots. As one can see, the

https://doi.org/10.1017/S0022377811000407 Published online by Cambridge University Press

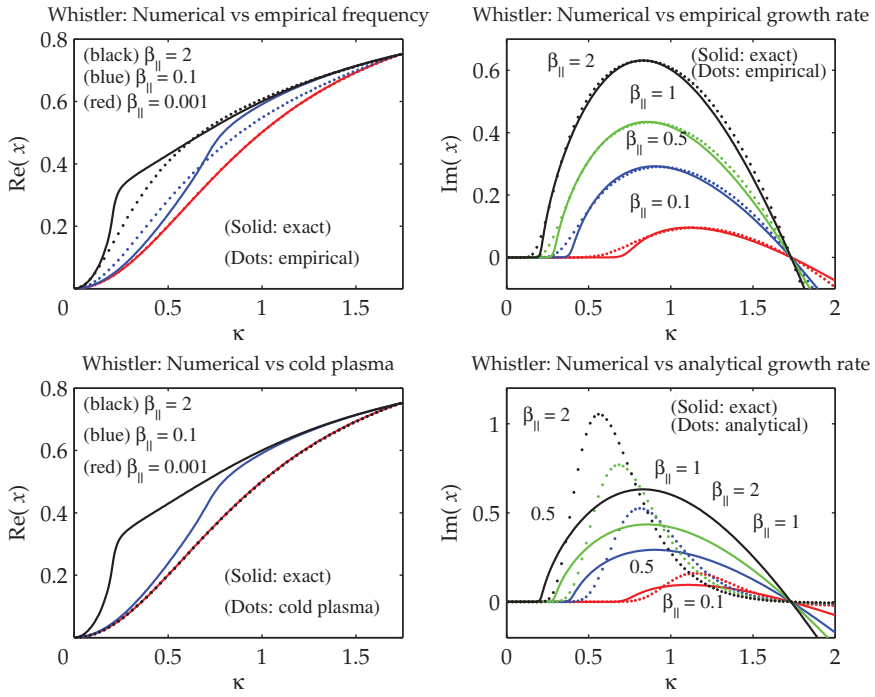


Figure 2. (Colour online) Whistler instability. (Top left): Comparison of exact numerical real frequency (solid lines), $\mathrm{Re}(x) = \omega/|\Omega_e|$, and empirical formula (dots) versus normalized wave number, $\kappa = ck/\omega_{pe}$, for anisotropy $A = T_\perp/T_\parallel - 1 = 3$ and for parallel betas, $\beta_\parallel = 8\pi n T_\parallel/B^2 = 0.001$ (red), 0.1 (blue), and 2 (black). (Top right): Comparison of exact numerical growth rate (solid lines), $\mathrm{Im}(x) = \gamma/|\Omega_e|$, and empirical formula (dots) versus normalized wave number, $\kappa = ck/\omega_{pi}$, for anisotropy $A = T_\perp/T_\parallel - 1 = 3$ and for parallel betas, $\beta_\parallel = 8\pi n T_\parallel/B^2 = 0.1$ (red), 0.5 (blue), 1 (green), and 2 (black). (Bottom left): Comparison of exact real frequency and cold-plasma dispersion relation (dots). Good agreement is found only for $\beta_\parallel = 0.001$. (Bottom right): Comparison of exact numerical growth rate (solid lines) and analytical growth rate (dots). Approximate Landau growth rate formula grossly overestimates the actual growth rate.

analytical growth rate formula grossly overestimates the actual wave growth.

As amply demonstrated by Figs. 1 and 2, our empirical formulae (2.5), (2.6), and (2.10) successfully model the actual solution, whereas the customary analytical growth rate and cold-plasma dispersion relations (2.7) and (2.11) are inadequate. However, as empirical models are not exact solutions, and small but non-negligible quantitative differences are bound to exist if one is to go beyond the linear stage of the instability, small initial differences in the linear growth may accrue to appreciable discrepancies in the wave amplitude since the waves amplify exponentially in time. To check whether such long time-scale difference may invalidate our empirical approach or not is not at all evident at the outset on the basis of intuition. We thus address this issue by performing quasilinear analysis based upon the empirical formula and comparing the outcome against numerical solution.

Before we present the present findings, we caution the readers of the limitation of our approach. Our empirical formulae as well as exact roots are strictly applicable only to bi-Maxwellian plasmas. In nonlinear stage of the instability, the particle distribution may substantially deviate from the assumed bi-Maxwellian form as a result of local distortion in the velocity space owing to local wave-particle resonance. However, if the instability involves the bulk of ions in resonance with waves, then the assumption of self-similarity may not be too bad. In any case, the purpose of the present paper is not to address the general nonlinear evolution of EMIC and whistler anisotropy instabilities but rather to verify whether the empirical approach is valid over long time-scale or not.

3. Quasilinear theory

3.1. General formulation

Let us define the adiabatic perpendicular and parallel temperatures by taking $v_\perp^2$ and v_z^2 moments of the particle distribution function $F_a(v_\perp^2, v_z, t)$,

$$T_{\perp a}(t) = \frac{m_a}{2}\int d\mathbf{v}\, v_\perp^2\, F_a\left(v_\perp^2, v_z, t\right),$$

$$T_{\parallel a}(t) = m_i \int d\mathbf{v}\, v_z^2\, F_a\left(v_\perp^2, v_z, t\right). \tag{3.1}$$

Following Davidson and Ogden (1975) and Yoon (1992), we assume that the particle distribution function F_a retains the self-similar form for all t, namely $F_a = G(v_\perp^2, t)\exp[-v_z^2/v_{Ta}^2(t)]/[\pi^{1/2}\, v_{Ta}(t)]$. We take the $v_\perp^2$ and v_z^2 moments of the quasilinear diffusion equation

$$\frac{\partial F_a}{\partial t} = -\mathrm{Im}\,\frac{e_a^2}{m_a^2}\int dk\,\frac{1}{v_\perp}\mathscr{D}\sum_{+,-}\frac{v_\perp \mathscr{E}_\pm(k)}{\omega - kv_z \pm \Omega_a}\mathscr{D}F_a,$$

$$\mathscr{D} = \frac{\omega - kv_z}{\omega}\frac{\partial}{\partial v_\perp} + \frac{kv_\perp}{\omega}\frac{\partial}{\partial v_z}, \tag{3.2}$$

https://doi.org/10.1017/S0022377811000407 Published online by Cambridge University Press

where $\mathscr{E}_{\pm}(k,t)$ is the spectral wave energy density associated with right-/left-hand modes. The corresponding wave kinetic equation is given by $\partial\mathscr{E}_{\pm}(k,t)/\partial t = 2\gamma_k(t)\,\mathscr{E}_{\pm}(k,t)$, where $\gamma_k(t)$ is the growth rate of the instability.

Upon taking the appropriate moments, we obtain the moment kinetic equations for perpendicular and parallel temperatures,

$$\frac{dT_{\perp a}}{dt} = \mathrm{Im}\,\frac{e_a^2}{2m_a}\sum_{+,-}\int\frac{dk}{|\omega|^2}\,\mathscr{E}_{\pm}(k) \times\left\{\omega^*\left[\xi\,Z(\zeta_{\pm})+\left(\frac{T_{\perp a}}{T_{\parallel a}}-1\right)[1+\zeta_{\pm}Z(\zeta_{\pm})]\right] - i\,\frac{T_{\perp a}}{T_{\parallel a}}\,\gamma_k - \left[\frac{T_{\perp a}}{T_{\parallel a}}\,\omega\mp\left(\frac{T_{\perp a}}{T_{\parallel a}}-1\right)\Omega_a\right] \times\zeta_{\pm}Z(\zeta_{\pm})\right\}, \tag{3.3}$$

$$\frac{dT_{\parallel a}}{dt} = -2\,\frac{dT_{\perp a}}{dt} + \mathrm{Im}\,\frac{e_a^2}{m_a}\sum_{+,-}\int\frac{dk}{|\omega|^2}\,\mathscr{E}_{\pm}(k)\,\omega^* \times\left[\xi\,Z(\zeta_{\pm})+\left(\frac{T_{\perp a}}{T_{\parallel a}}-1\right)[1+\zeta_{\pm}Z(\zeta_{\pm})]\right],$$

where $\xi = \omega/kv_{Ta}$ and $\zeta_{\pm} = (\omega\mp\Omega_a)/k_z v_{Ta}$. The above moment kinetic equations are to be solved together with the instantaneous dispersion relation at each time-step along the quasilinear evolution of the instability.

3.2. Quasilinear evolution of EMIC instability

For EMIC instability we choose only the contribution from the left-hand mode in (3.3). Upon making use of the instantaneous dispersion relation, we may simplify (3.3) for the ions,

$$\frac{dT_{\perp i}}{dt} = -\frac{e^2}{2m_i}\int\frac{dk}{|\omega|^2}\,\mathscr{E}(k)\left\{\gamma_k\left(\frac{c^2k^2}{\omega_{pi}^2}+\frac{T_{\perp i}}{T_{\parallel i}}\right) + \mathrm{Im}\left[\omega+\left(\frac{T_{\perp i}}{T_{\parallel i}}-1\right)(\omega-\Omega_i)\right]\zeta\,Z(\zeta)\right\},$$

$$\frac{dT_{\parallel i}}{dt} = -2\,\frac{dT_{\perp i}}{dt} - \frac{e^2}{m_i}\int\frac{dk}{|\omega|^2}\,\gamma_k\,\mathscr{E}(k)\,\frac{c^2k^2}{\omega_{pi}^2}, \tag{3.4}$$

where $\xi = \omega/kv_{Ti}$ and $\zeta = (\omega-\Omega_i)/k_z v_{Ti}$. Besides the dimensionless quantities already encountered, namely $\beta_{\perp} = 8\pi nT_{\perp i}/B^2$, $\beta_{\parallel} = 8\pi nT_{\parallel i}/B^2$, $A = T_{\perp i}/T_{\parallel i} - 1 = \beta_{\perp}/\beta_{\parallel} - 1$, $x = \omega/\Omega_i$, $\kappa = k_z v_A/\Omega_i = ck_z/\omega_{pi}$, we adopt the following additional normalization scheme:

$$\tau = \Omega_i t, \quad \mathscr{W}(\kappa,\tau)\,d\kappa = \frac{c^2}{v_A^2}\,\frac{\kappa^2}{|x|^2}\,\frac{\mathscr{E}(k,t)}{B^2}\,dk = \frac{\delta B_k^2}{B^2}\,dk. \tag{3.5}$$

In terms of the normalized variables and quantities, moment kinetic equations for ion betas can be expressed as follows:

$$\frac{d\beta_{\perp}}{d\tau} = -\int\frac{d\kappa}{\kappa^2}\,\mathscr{W}(\kappa,\tau)[x_i(\kappa^2+A+1) + \mathrm{Im}\,(x-A+xA)\,\zeta\,Z(\zeta)],$$

$$\frac{d\beta_{\parallel}}{d\tau} = -2\,\frac{d\beta_{\perp}}{d\tau} - 2\int d\kappa\;x_i\,\mathscr{W}(\kappa,\tau), \tag{3.6}$$

together with the wave kinetic equation, $\partial\mathscr{W}(\kappa,\tau)/\partial\tau = 2x_i\,\mathscr{W}(\kappa,\tau)$. In (3.6), $\zeta = (x-1)/\kappa\beta_{\parallel}^{1/2}$ and $x = \mathrm{Re}\,(x) + i\,\mathrm{Im}\,(x) = x_r + x_i$, x_r and x_i being the normalized real frequency and the growth rate, respectively. The standard quasilinear analysis developed by Davidson and Ogden (1975) solves the instantaneous (or adiabatic) dispersion relation (2.2) at each time along the quasilinear evolution of the system. The method based upon the empirical dispersion relation bypasses this step by making use of the analytical expression for $\mathrm{Re}\,(x) = x_r$ and $\mathrm{Im}\,(x) = x_i$ as given by (2.5) and (2.6). In what follows, we shall carry out numerical analysis based upon both approaches and compare the outcome.

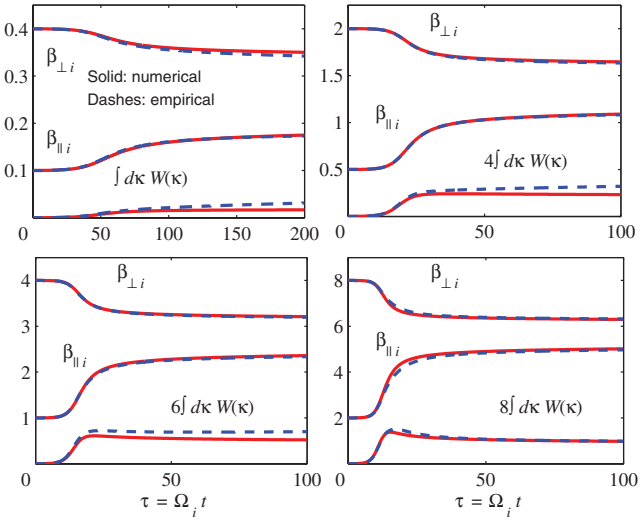


Figure 3. (Colour online) Time evolution of normalized perpendicular and parallel temperatures, $\beta_{\perp i}(t) = 8\pi nT_{\perp i}(t)/B^2$ and $\beta_{\parallel i}(t) = 8\pi nT_{\parallel i}(t)/B^2$, respectively, as well as normalized spectral wave energy density $\int dk\;\mathscr{W}(k,t) = (\delta B)^2(t)/B^2$ versus normalized time $\tau = \Omega_i t$, for initial temperature anisotropy factor $A = T_{\perp i}/T_{\parallel i} - 1 = 3$ and initial parallel ion betas corresponding to (a) $\beta_{\parallel i}(0) = 0.1$; (b) $\beta_{\parallel i}(0) = 0.5$; (c) $\beta_{\parallel i}(0) = 1.0$; and (d) $\beta_{\parallel i}(0) = 2.0$.

For the present purpose, we consider initial temperature anisotropy factor $A = 3$ or equivalently, $T_{\perp i}(0)/T_{\parallel i}(0) = \beta_{\perp}(0)/\beta_{\parallel}(0) = 4$, and a range of parallel ion betas, $\beta_{\parallel} = 0.1$, 0.5, 1.0, and 2.0. The initial wave energy density $\mathscr{W}(\kappa,0)$ is arbitrarily chosen as $\mathscr{W}(\kappa,0) = \delta B_k^2(0)/B^2 = 0.01$. Figure 3 compares numerical solutions based on solving adiabatic dispersion relation by numerical means (solid lines), and that based upon empirical dispersion relation (2.5) and (2.6) (dashes). Plotted in each panel are perpendicular and parallel ion betas, $\beta_{\perp}$ and $\beta_{\parallel}$ (or normalized perpendicular and parallel temperatures, $8\pi nT_{\perp i}/B^2$ and $8\pi nT_{\parallel i}/B^2$) and

https://doi.org/10.1017/S0022377811000407 Published online by Cambridge University Press

normalized wave energy density $\int d\kappa\ \mathscr{W}(\kappa,\tau)$, respectively, versus normalized time $\tau = \Omega_i t$. The initial temperature anisotropy factor is $A = 3$ and initial parallel ion betas are $\beta_\parallel = 0.1$, 0.5, 1.0, and 2.0, respectively. The four cases of different initial parallel betas are plotted in panels (a) to (d). Note that the agreement between the exact numerical versus empirical methods is quite good. Also note that the agreement is better for high initial parallel betas, although the differences between varying initial betas are marginal.

3.3. *Quasilinear evolution of whistler instability*

For the right-hand whistler instability we ignore the contribution from the left-hand mode in (3.3) and make use of instantaneous dispersion relation

$$\frac{c^2k^2}{\omega_{pe}^2} = \xi\, Z(\zeta) + \left(\frac{T_{\perp e}}{T_{\parallel e}} - 1\right)[1 + \zeta\, Z(\zeta)], \qquad (3.7)$$

where $\xi = \omega/kv_{Te}$ and $\zeta = (\omega - |\Omega_e|)/k_z v_{Te}$, to obtain

$$\frac{dT_{\perp e}}{dt} = -\frac{e^2}{2m_e}\int \frac{dk}{|\omega|^2}\,\mathscr{E}(k)\left\{\gamma_k\left(\frac{c^2k^2}{\omega_{pe}^2} + \frac{T_{\perp e}}{T_{\parallel e}}\right)\right.$$
$$\left. + \mathrm{Im}\left[\frac{T_{\perp e}}{T_{\parallel e}}\,\omega - \left(\frac{T_{\perp e}}{T_{\parallel e}} - 1\right)|\Omega_e|\right]\zeta\, Z(\zeta)\right\},$$

$$\frac{dT_{\parallel e}}{dt} = -2\,\frac{dT_{\perp e}}{dt} - \frac{e^2}{m_e}\int \frac{dk}{|\omega|^2}\,\gamma_k\,\mathscr{E}(k)\,\frac{c^2k^2}{\omega_{pe}^2}. \qquad (3.8)$$

Upon making use of dimensionless quantities, $\beta_\perp = 8\pi n T_{\perp e}/B^2$, $\beta_\parallel = 8\pi n T_{\parallel e}/B^2$, $A = T_{\perp e}/T_{\parallel e} - 1$, $x = \omega/|\Omega_e|$, $\kappa = ck/\omega_{pe}$, and

$$\tau = |\Omega_e|\,t, \quad \mathscr{W}(\kappa,\tau)\,d\kappa = \frac{\omega_{pe}^2}{\Omega_e^2}\,\frac{\kappa^2}{|x|^2}\,\frac{\mathscr{E}(k,t)}{B^2}\,dk = \frac{\delta B_k^2}{B^2}\,dk, \qquad (3.9)$$

one finds that (3.8) is in exactly the same mathematical expression as the normalized (3.6). We thus proceed to discuss sample numerical examples below.

For the whistler anisotropy instability, we consider initial temperature anisotropy factor as in the previous case for EMIC instability, namely $A = 3$ or equivalently, $T_{\perp e}(0)/T_{\parallel e}(0) = 4$, and a range of parallel electron betas, $\beta_\parallel = 0.1$, 0.2, 0.5, and 1.0. The initial wave energy density $\mathscr{W}(\kappa,0)$ is arbitrarily chosen as $\mathscr{W}(\kappa,0) = \delta B_k^2(0)/B^2 = 0.01$. Figure 4 compares numerical solutions based on adiabatic dispersion relation and that based upon empirical dispersion relation (2.10) (dashes). As one can see, the agreement between the exact numerical versus empirical methods is quite reasonable just as in the case of EMIC instability.

As is well known, complete isotropy cannot be achieved within quasilinear treatment of temperature anisotropy instabilities. (Complete isotropization in collisionless plasmas is generally not possible.) Nonetheless, the important point in Figs. 3 and 4 is to demonstrate that the empirical method of computing EMIC and whistler anisotropy instability dispersion relations and growth rates leads to an overall agreement with that based upon rigorous numerical root solving scheme,

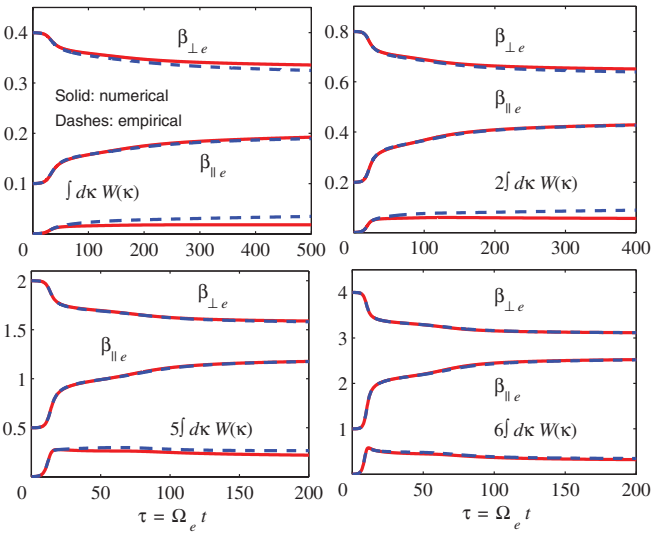


Figure 4. (Colour online) Time evolution of normalized perpendicular and parallel temperatures, $\beta_{\perp e}(t) = 8\pi n T_{\perp e}(t)/B^2$ and $\beta_{\parallel e}(t) = 8\pi n T_{\parallel e}(t)/B^2$, respectively, as well as normalized spectral wave energy density $\int d\kappa\ \mathscr{W}(k,t) = (\delta B)^2(t)/B^2$ versus normalized time $\tau = |\Omega_e|t$ for initial temperature anisotropy factor $A = T_{\perp e}/T_{\parallel e} - 1 = 3$ and initial parallel electron betas corresponding to (a) $\beta_{\parallel e}(0) = 0.1$; (b) $\beta_{\parallel e}(0) = 0.2$; (c) $\beta_{\parallel e}(0) = 0.5$; and (d) $\beta_{\parallel e}(0) = 1.0$.

which proves that the present shortcut method can be reasonably reliable and that it does not lead to an accumulated error over long time, a conclusion that could not have been predicted at the outset.

4. Discussion and conclusions

In the present paper we have made use of the recently developed empirical linear dispersion theory for anisotropy-driven EMIC and whistler instabilities (Seough and Yoon 2009; Yoon et al. 2010, 2011), and applied the formalism to quasilinear evolution of these instabilities. As Figs. 1–4 show, the comparison between the exact numerical method and the present method based upon empirical method show reasonable agreement.

The significance of the present paper in the context of the geophysical application may be in the radiation belt transport problem. As is well known, EMIC waves are thought to be an important loss mechanism for relativistic electrons in the radiation belt, whereas the whistler chorus waves are thought to be responsible for energizing relativistic electrons as well as for their pitch-angle scattering. Quasilinear kinetic theory has been one of the most important research tools in that regard. However, one of the key assumptions in the literature (Kennel and Petschek 1966; Lyons et al. 1972; Schulz and Lanzerotti 1974; Summers and Ma 2000; Summers and Thorne 2003; Albert 2005; Glaubert and Horne 2005; Summers 2005; Summers et al. 2007; Xiao et al. 2010) is that the background plasma is cold, even though the radiation belt and the ring current

https://doi.org/10.1017/S0022377811000407 Published online by Cambridge University Press

can attain high betas (of the order of 0.1 or higher) during storm times, and that warm plasma effects can significantly alter the basic dispersive properties of the waves.

Our recent works (Seough and Yoon 2009; Yoon et al. 2010, 2011) open the possibility of incorporating warm plasma effects into the radiation belt transport calculation for the first time. The closed-form analytical nature associated with our empirical dispersion formulae makes such efforts possible. Before we do that, however, it is important to verify the reliability of our formulae, particularly over the course of long-time instability development. The question we aimed to address in the present paper is whether the empirical growth rate formula will lead to an accumulated error over long time-scale or not. We addressed this issue by performing quasilinear analysis on the basis of empirical formula versus more rigorous method. We find, to our satisfaction, that the empirical heuristic dispersion formulae stood the test rather remarkably.

Before we close, however, we should note that natural space plasmas generally display a pronounced non-Maxwellian high energy tail distribution that can be well modeled by a generalized Lorentzian (or kappa) distribution, and that the instability characteristics of kappa distribution can be quantitatively different from that of bi-Maxwellian distributions (e.g. Xiao 2006, Xiao et al. 2006, 2007). In this sense, the present analysis of quasilinear anisotropy instabilities based on the bi-Maxwellian model may be limited. However, we hasten to point out that the purpose of the present paper is to test whether empirical models will lead to an accumulated error along time-scale or not, which has been properly achieved with the bi-Maxwellian model. In the future, however, it will be not only interesting but important to extend the present paper to the generalized Lorentzian (or kappa) model.

Acknowledgments

This research was supported by WCU grant R31-10016 from the Korean Ministry of Education, Science and Technology.

References

Albert, J. M. 2005 Evaluation of quasi-linear diffusion coefficients for whistler mode waves in a plasma with arbitrary density ratio. *J. Geophys. Res.* **110**, A03218.

Cuperman, S., Gomberoff, N. L. and Sternlieb, A. 1975 Absolute maximum growth rates and enhancement of unstable electromagnetic ion-cyclotron waves in mixed warm-cold plasmas. *J. Plasma Phys.* **13**, 259.

Davidson, R. C. and Ogden, J. M. 1975 Electromagnetic ion cyclotron instability driven by ion energy anisotropy in high-beta plasmas. *Phys. Fluids* **18**, 1045.

Glaubert, S. A. and Horne, R. B. 2005 Calculation of pitch angle and energy diffusion coefficients with the PADIE code. *J. Geophys. Res.* **110**, A04206.

Kennel, C. F. and Petschek, H. E. 1966 Limit on stably trapped particle flux. *J. Geophys. Res.* **71**, 1.

Krall, N. A. and Trivelpiece, A. W. 1973 *Principles of Plasma Physics*. New York, NY: McGraw-Hill.

Lui, A. T. Y., McEntire, R. W. and Krimigis, S. M. 1987 Evolution of the ring current during two geomagnetic storms. *J. Geophys. Res.* **92**, 7459.

Lyons, L. R., Thorne, R. M. and Kennel, C. F. 1972 Pitch-angle diffusion of radiation belt electrons within the plasmasphere. *J. Geophys. Res.* **77**, 3455.

Schulz, M. and Lanzerotti, L. J. 1974 *Particle Diffusion in the Radiation Belts, Physics and Chemistry in Space*, Vol. 7. New York: Springer-Verlag.

Seough, J. J. and P. H. Yoon 2009 Analytic models of warm plasma dispersion relations. *Phys. Plasmas* **16**, 092103.

Summers, D. 2005 Quasi-linear diffusion coefficients for field-aligned electromagnetic waves with applications to the magnetosphere. *J. Geophys. Res.* **110**, A08213.

Summers, D. and Ma, C. 2000 A model for generating relativistic electrons in the Earth's inner magnetosphere based on gyroresonant wave-particle interactions. *J. Geophys. Res.* **105**, 2625.

Summers, D. and Thorne, R. M. 2003 Relativistic electron pitch-angle scattering by electromagnetic ion cyclotron waves during geomagnetic storms. *J. Geophys. Res.* **108**(A4), 1143.

Summers, D., Ni, B. and Meredith, N. P. 2007 Timescales for radiation belt electron acceleration and loss due to resonant wave-particle interactions: 1. Theory. *J. Geophys. Res.* **112**, A04206, A04207.

Xiao, F. 2006 Modelling energetic particles by a relativistic kappa-loss-cone distribution function in plasmas. *Plasma Phys. Control. Fusion* **48**, 203.

Xiao, F., Zhou, Q., Zheng, H. and Wang, S. 2006 Whistler instability threshold condition of energetic electrons by kappa distribution in space plasmas. *J. Geophys. Res.* **111**, A08208.

Xiao, F., Zhou, Q., He, H., Zheng, H. and Wang, S. 2007 Electromagnetic ion cyclotron waves instability threshold condition of suprathermal protons by kappa distribution. *J. Geophys. Res.* **112**, A07219.

Yoon, P. H. 1992 Quasilinear evolution of Alfvén-ion-cyclotron and mirror instabilities driven by ion temperature anisotropy. *Phys. Fluids* B **4**, 3627.

Yoon, P. H., Seough, J. J., Khim, K. K., Kim, H., Kwon, H.-J., Park, J., Parkh, S. and Park, K. S. 2010 Analytic model of electromagnetic ion-cyclotron anisotropy instability. *Phys. Plasmas* **17**, 082111.

Yoon, P. H., Seough, J. J., Lee, J., An, J. and Lee, J. O. in press Empirical model of whistler anisotropy instability. *Phys. Plasmas* (submitted).

https://doi.org/10.1017/S0022377811000407 Published online by Cambridge University Press